

Notes on boson stars in scalar-tensor theory and code infrastructure

Tamara Evstafyeva

1 Theory action

In the Einstein frame

$$S_E = \frac{1}{16\pi G} \int dx^4 \sqrt{-\bar{g}} \{ \bar{R} - 2\bar{g}^{\mu\nu} \partial_\mu \varphi \partial_\nu \varphi - 4W(\varphi) \} + S_m[\psi_m, F(\varphi)^{-1} \bar{g}_{\mu\nu}]. \quad (1.1)$$

In the Jordan, aka physical, frame

$$S_J = \int dx^4 \sqrt{-g} \left\{ \frac{F(\phi)}{16\pi G} R - \frac{1}{2} g^{\mu\nu} \partial_\mu \phi \partial_\nu \phi - U(\phi) \right\} + S_m(\psi_m, g_{\mu\nu}), \quad (1.2)$$

where in the physical frame the matter counterpart is given via a bosonic action

$$S_m = \int dx^4 \sqrt{-g} \left\{ -\frac{1}{2} [g^{\mu\nu} \nabla_\mu \psi^* \nabla_\nu \psi + V(\psi)] \right\}. \quad (1.3)$$

2 Variables

To avoid confusion, I have mainly used the variables of Uli's notes, i.e.

- A – amplitude of the bosonic scalar field.
- ω – frequency of the boson star, in the code we start with initial guess of $\omega = 1$, but this can be changed if searching for other solutions.
- φ – gravitational scalar field.
- α – lapse function.
- X – function of r from line-element ansatz $ds^2 = -\alpha^2 dt^2 + X^2 dr^2 + \frac{r^2}{F} d\Omega^2$.
- $W(\varphi)$ – potential function for the gravitational scalar field given by $W(\varphi) = \frac{1}{2} \mu_\varphi^2 \varphi^2$, where μ_φ^2 is the mass variable.
- $V(A^2)$ – solitonic potential for the bosonic scalar field defined by $V(A^2) = A^2 \left(1 - 2 \frac{A^2}{\sigma_0^2} \right)^2$.
- $F(\varphi)$ – conformal factor defined by $F(\varphi) = e^{-2\alpha_0 \varphi - \beta_0 \varphi^2}$.

To have only first order derivatives, we further introduce the following auxiliary variables

$$\partial_r \varphi = X\eta, \quad (2.1)$$

$$\partial_r A = \Psi_0. \quad (2.2)$$

We also choose to use Φ instead of the lapse α , which is defined as

$$\Phi = \ln \left(\sqrt{F} \alpha \right). \quad (2.3)$$

Finally, we note that

$$\frac{\partial_r F}{F} = \frac{F_{,\varphi}}{F} \partial_r \varphi = \frac{F_{,\varphi}}{F} X\eta. \quad (2.4)$$

3 Equations of integration

Below we detail the equations that we implement for outward integration in the code. Note that the set of variables we are solving for is given by $\{\Phi, X, \eta, \Psi_0\}$.

$$\partial_r \Phi = \frac{FX^2 - 1}{2r} - rFX^2W + \frac{r}{2}(X\eta)^2 + 2\pi r \frac{X^2}{F} \left[\frac{\Psi_0^2}{X^2} + \frac{A^2\omega^2}{\alpha^2} - V \right], \quad (3.1)$$

$$\frac{\partial_r X}{X} = -\frac{FX^2 - 1}{2r} + rFX^2W - \frac{1}{2} \frac{F_{,\varphi}}{F} X\eta + \frac{r}{2}(X\eta)^2 + 2\pi r \frac{X^2}{F} \left[\frac{\Psi_0^2}{X^2} + \frac{A^2\omega^2}{\alpha^2} + V \right] \quad (3.2)$$

$$\partial_r \eta = -\eta \left(\partial_r \Phi - \frac{1}{2} \frac{F_{,\varphi}}{F} X\eta \right) - \frac{2}{r} \eta + FXW_{,\varphi} + \frac{2\pi XF_{,\varphi}}{F^2} \left[\frac{A^2\omega^2}{\alpha^2} - \frac{\Psi_0^2}{X^2} - 2V \right], \quad (3.3)$$

$$\partial_r \Psi_0 = -2 \frac{\Psi_0}{r} + \Psi_0 \left(\frac{\partial_r X}{X} + \frac{3}{2} \frac{\partial_r F}{F} - \partial_r \Phi \right) - \frac{X^2 \omega^2 A}{\alpha^2} + X^2 V_{,|\psi|^2} A, \quad (3.4)$$

where I was lazy to replace $\alpha \rightarrow e^\Phi/\sqrt{F}$.

4 Boundary conditions at the origin

At $r = 0$, the boundary condition are

$$\partial_r \varphi(r = 0) = 0 \implies \eta(r = 0) = 0, \quad (4.1)$$

$$\partial_r A(r = 0) = 0, \quad (4.2)$$

$$\Phi(r = 0) = 0, \quad (4.3)$$

$$A(r = 0) = A_c \quad (\text{user-specified}), \quad (4.4)$$

$$X(r = 0) = \frac{1}{\sqrt{F(\varphi(0))}}, \quad (4.5)$$

$$\varphi(r = 0) = \varphi_c \quad (\text{user-specified but is checked and improved until surface condition is satisfied}). \quad (4.6)$$

5 Series expansion near the origin

Using the boundary condition at the origin (4.6), we are able to derive the behaviour of our PDEs at the origin, which in the code are implemented within an open ball of small

radius ($r_{\text{small}} = 10^{-15}$)

$$\partial_r \Phi = 0, \quad (5.1)$$

$$\partial_r X = 0, \quad (5.2)$$

$$\partial_r \Psi_0 = \frac{1}{3} \left(\frac{1}{F} V_{,|\psi|^2} A - \omega^2 A e^{-2\Phi} \right), \quad (5.3)$$

$$\partial_r \eta = \frac{1}{3} \left[\sqrt{F(\varphi(0))} W_{,\varphi} + \frac{2\pi F_{,\varphi}}{F^2 \sqrt{F}} \left(\frac{\omega^2 A^2 F}{e^{2\Phi}} - 2V \right) \right]. \quad (5.4)$$

6 Conversion to isotropic radius

If one prefers to work with isotropic radius, here we present how their radial quantities are related. This is also coded up in the 1D-solver. I'd expect the isotropic line-element ansatz for the scalar-tensor theory would take the following form

$$ds^2 = -F\alpha^2 dt^2 + F\psi^4 (dR^2 + R^2 d\Omega^2). \quad (6.1)$$

Comparing it with the areal-radius line-element, which is assumed to be

$$ds^2 = -F\alpha^2 dt^2 + FX^2 dr^2 + r^2 d\Omega^2, \quad (6.2)$$

we find the following relations between the variables

$$F\psi^4 R^2 = r^2 \quad \text{and} \quad \psi^4 dR^2 = X^2 dr^2. \quad (6.3)$$

The latter equation has a singular nature, making our lives harder, so in order not to deal with singularities, we introduce a new variable

$$f(r) := \frac{R}{r} \quad \implies \quad \frac{df}{dr} = \frac{f}{r} (X\sqrt{F} - 1). \quad (6.4)$$

At the origin, we know that $X(r=0) = 1/\sqrt{F(\varphi(0))} + \mathcal{O}(r^2)$ and so in the derivative equation for $f(r)$, (6.4), the bracket becomes zero and the radii relate linearly, in other words $R \propto r$. In the code, we therefore set $f = 1$ initially and integrate it out; after that we re-scale it appropriately by requiring that both radii agree at infinity. We can do this, since any kind of multiplication of the solution by a constant still gives us the solution to the ODE.

Now, to find this appropriate re-scaling to the $f(r)$ solution, we equate the areas resulted from the line-elements (6.1)–(6.2) and for large radii approximate the conformal factor of the isotropic line-element via $\psi = 1 - m/(2R)$. By doing so the equality simplifies to the following

$$r^2 = F \left(1 - \frac{m}{2R} \right)^4 R^2. \quad (6.5)$$

After some algebraic manipulations, we then obtain the following radial relations

$$R = \left(\frac{r}{\sqrt{F}} - m \right) - \frac{1}{4} \frac{\sqrt{F} m^2}{\left(r - \sqrt{F} m \right)} \quad \Leftrightarrow \quad r = \sqrt{F} \left(m + R + \frac{1}{4} \frac{m^2}{R} \right), \quad (6.6)$$

which reduce to the GR case in the limit, $F \rightarrow 1$ (see Uli's notes on BSs).

7 Asymptotic behaviour

Whilst the asymptotics turned quite out tricky and we have identified 3 cases that should be analysed separately for when $\alpha_0 \neq 0$ (with 2 of them being 'physical'). We focus on the case when $h < 2k$, which forces most of the 'nasty' terms to cancel in the asymptotic behaviour of the equations. This means the asymptotic behaviours of the bosonic scalar field and the gravitational scalar field are summarized as follows

$$\varphi \sim \frac{e^{-hr}}{r^{1+\delta}}, \quad \text{where } h = m \quad \text{and} \quad \delta = Mm = Mh, \quad (7.1)$$

$$A \sim \frac{e^{-kr}}{r^{1+\epsilon}}, \quad \text{where } k = \sqrt{1 - \omega^2} \quad \text{and} \quad \epsilon = M \frac{1 - 2\omega^2}{k} = M \frac{2k^2 - 1}{k}, \quad (7.2)$$

where we estimate the mass M using the mass function $m(r) := \frac{r}{2} \left(1 - \frac{1}{FX^2}\right)$ and the frequency ω through the shooting algorithm. It is crucial to note that we also need to reinforce that the lapse function goes to unity at infinity, that is $\lim_{r \rightarrow \infty} \alpha = 1$. We can re-scale α (or Φ in our case), as long as we re-scale ω with it! This is achieved via $\omega \rightarrow \omega e^{-\ln(\sqrt{FX}) - \ln(\sqrt{F}\alpha)}$.

8 Methodology for the massless case

The idea is pretty much the same as for our 'classic' boson stars. Briefly, this means that we take our equations (3.1)–(3.4) and integrate them outwards until some r_{stop} , where the solution for the bosonic field diverges and goes bonkers. From r_{stop} we set the bosonic variable counterparts to zero to avoid crashing the code. We then find the minimum of the bosonic scalar field before it starts to diverge, and glue the asymptotic behavior to it.

We concentrate on the *massless* case for the time being, and in this case we do not use the asymptotic behavior for φ , as it is super slow, but rather just continue integrating outwards the equation for the gravitational scalar field. We repeat the whole integration from the point of asymptotic matching, now hopefully getting a physical solution.

Usually any initial guess for φ_c produces something. However, is it what we are looking for? Sadly, not really. To enforce 'the correct solution' in the code, we use the surface condition equation for the gravitational scalar field by Damour [1, 2]. It is in principle applicable to vacuum, however far away (at large radius) the boson star is fairly 'vacuum', we assume it is alright for us approximation to use. The condition gives the expected value for the gravitational scalar field on the surface of the star, or just 'far enough' for our case

$$\varphi_s = -\frac{X_s \eta_s}{\sqrt{(\partial_r \Phi_s)^2 + X_s \eta_s}} \operatorname{artanh} \frac{\sqrt{(\partial_r \Phi_s)^2 + X_s \eta_s}}{\partial_r \Phi_s + 1/r_s}. \quad (8.1)$$

Here by 's' we denote the variable evaluated on the star's surface. In our code the surface is defined as just a few gridpoints away from the edge of the grid. We quantify how well this condition is satisfied by comparing it with our numerical value for φ at that surface

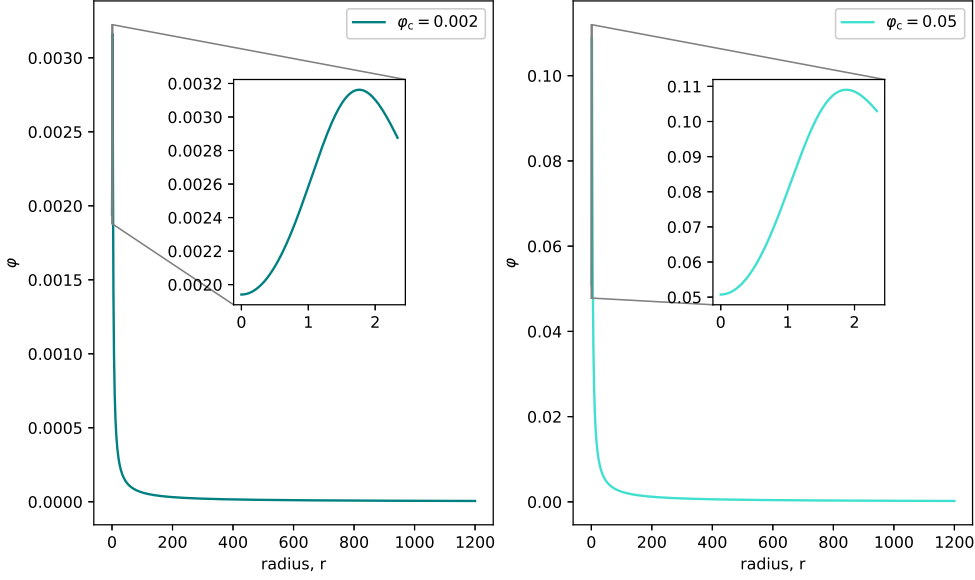


Figure 1: Profile of the gravitational scalar field as a function of the radius, computed from different initial guesses for φ_c . One yields a profile of roughly $\mathcal{O}(\alpha)$, whereas the other one results in much more scalarisation giving $\varphi \sim \mathcal{O}(1)$; the asymptotic condition is satisfied for both cases.

point, and improve on the central field guess φ_c until we meet this surface condition up to some satisfactory tolerance (i.e. 10^{-5}) using Newton-Raphson algorithm.

8.1 Example profile: massless case

Typically, with *very* negative values of β_0 , e.g. $\beta_0 = -12.0$, we can find strongly scalarised solutions. As an example for illustration purposes, let us choose $\beta_0 = -12$, $\alpha_0 = 0.01$ and $A_c = 0.147$. In this case, as illustrated in Fig. 1, it is possible to recover weakly and strongly scalarised solutions, depending on the central guess for the gravitational scalar field.

8.2 Convergence

We have investigated the convergence for the gravitational scalar field, φ , by setting a up a grid of radius 1200 and by taking 128001, 384003 and 1024001 number of points for low, medium and high resolutions correspondingly. Below, Figure 2, shows that we achieve 4th order of convergence through the whole profile of the scalar field. We utilise the number of points for low resolution in subsequent results we present below.

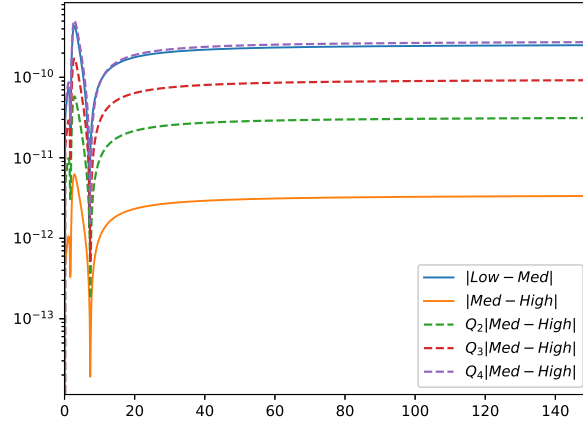


Figure 2: Convergence plot for the massless case, where Q_i for $i = 2, 3, 4$ stand for the re-scaling factor for the respective convergence rates.

9 Methodology for the massive case

The way the code works for the massive code is a little different, and it is in fact coded in a separate file. The equations and assumed asymptotic behaviour are all the same, except for 2 main principle features.

1. Both scalar fields now are matched to their corresponding asymptotic behaviours as in Eqs. (7.2)–(7.1). This matching to asymptotics happens in the following way. We find the diverging behavior of the fields at some finite radius and then search backwards for the local minimum. We then take 90% buffer region from the point of local minimum – this consequently defines our matching radius r_{match} . The points where bosonic scalar field and gravitational scalar fields have to be matched usually occur at different radii; sometimes they lie closely to each other.
2. The stopping criteria in the form of Eq. (8.1) is now swapped for an alternative condition to ensure that the matching is smooth. This is inspired by how the massless case is handled via Eqs. (3.40)–(3.41) of Ref. [3]. We recall that asymptotically the gravitational field behaves like

$$\varphi = Br^{-1-\delta}e^{-m_\varphi r}, \quad (9.1)$$

where B is some constant. Differentiating this expression, we obtain

$$\varphi'(r) = Br^{-2-\delta}e^{-m_\varphi r}(-1 - \delta - rm_\varphi), \quad (9.2)$$

which gives us a readily available expression for what B is

$$B = \frac{\varphi'(r)}{-1 - \delta - rm_\varphi} r^{2+\delta} e^{m_\varphi r}. \quad (9.3)$$

Now, the most common issue in the shooting, when finding a suitable solution for the gravitational scalar field, is having the field falling off too fast. In such scenarios, the radius of matching often appears to be too small; so when we glue the solution at that radius to the asymptotic expression, the solution does not look smooth enough. By ensuring that Eq. (9.1) is satisfied at the radius of matching r_{matching} to some user-specified threshold (e.g. 10^{-4}), we hope that the solver converges to some solution. If the computed $\varphi(r_{\text{matching}})$ is not the expected value, then we change the initial value of the gravitational scalar field $\varphi(0)$ and repeat the whole procedure until the threshold requirement is met. Once this criterion is reached, the matching looks smooth.

9.1 Zero-crossings of the gravitational scalar field

We already know that $A(r)$ has n number of zero crossings, which is quantised by the respective oscillation frequencies ω_n ; furthermore, the number of zero-crossings is a non-decreasing function of frequency, ω . Could there be a similar effect for the behavior of the gravitational scalar field, where now its central value φ_c determines the number of crossings?

To explore such possibility, we shoot for the frequency of the boson star ω and limit ourselves to the ground states only. Once we find appropriate frequency, we integrate the governing equations, without matching the fields' behaviours to their asymptotics. We do set the fields to zero at some fixed radius, when they start to diverge – this produces spikes in profiles but the behavior before these spikes is valuable for understanding the nature of zero-crossings of the gravitational scalar field.

Using the condition for smooth matching of Section 9 we find the central value of the gravitational scalar field that produces a smooth solution, which we also hope is the physical one. This profile is presented in blue in Fig. 3. We see that it falls off sufficiently slow (never crossing the x -axis) and reaches small positive values, but then at some larger radius ($r \sim 55$) starts to diverge. When we match this solution to its asymptotics, as expected, it then produces a smooth profile – yay! Now, what happens as we depart away from this central value and how does it affect the zero-crossings? The results shown in Fig. 3 suggest that similarly to the bosonic case, the number of zero crossings of the gravitational field increases or at least stays the same with increased central value φ_c . To be more precise, I only found cases where the gravitational scalar field never crosses the x -axis or crosses them once! The desired, smooth solution (in blue) appears to be the only 'viable' choice for asymptotic matching. All other guesses for φ_c around it produce profiles that either have one zero-crossing or diverge from a small radius.

The role of the central amplitude for the gravitational scalar field is therefore not totally equivalent to the bosonic ω and the number of crossings for the gravitational field is limited to one at maximum.

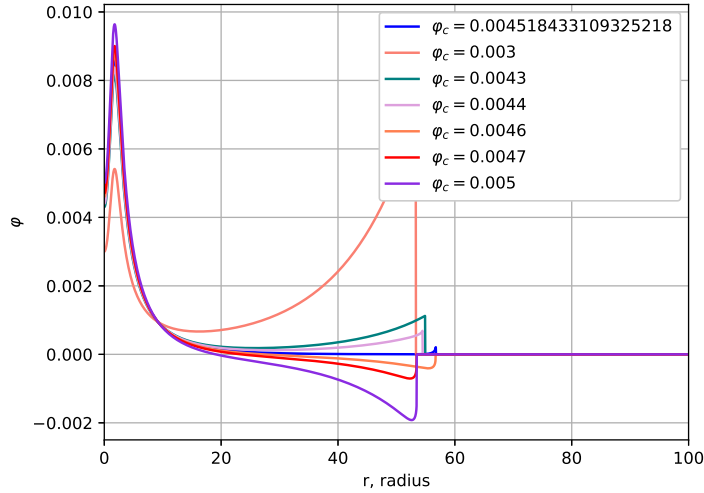


Figure 3: Profile of the gravitational scalar field found by shooting for ω and integrating out the equations without any asymptotic matching. The fields are set to zero when their amplitudes become large, and this is where the profiles produce spikes, which suddenly drop to zero.

9.2 Example profile: massive case

We now present some solutions for the massive case. Similarly to 8.1 we set $A_c = 0.147$, $\beta_0 = -12.0$, $\alpha = 0.01$ and see what happens... Here we choose $m_\varphi = 0.1$. As illustrated in Fig. 4, we can find a solution.

9.3 Convergence

We have investigated the convergence for the gravitational scalar field, φ , by setting up a grid of radius 1200 and by taking 524004, 768006 and 1024001 number of points for low, medium and high resolutions correspondingly. Below, Figure 5, shows that we achieve 4th order of convergence for small radii, which then drops down to 3rd order of convergence after the radius of asymptotic matching. We utilise the number of points for low resolution in subsequent results we present below.

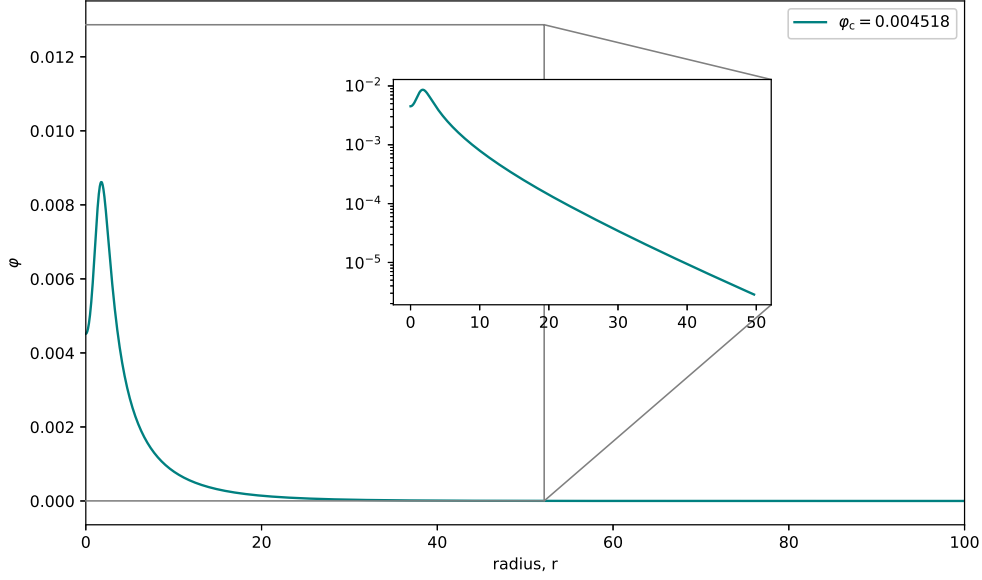


Figure 4: Profile of the gravitational scalar field as a function of the radius, computed from different initial guesses for φ_c for the massive case. The threshold for satisfying (9.1) has been chosen empirically making sure that matching is 'smooth'. The inset includes the zoom-in onto the profile on logarithmic scale, clearly demonstrating that there are no 'kinks' in our matching procedure.

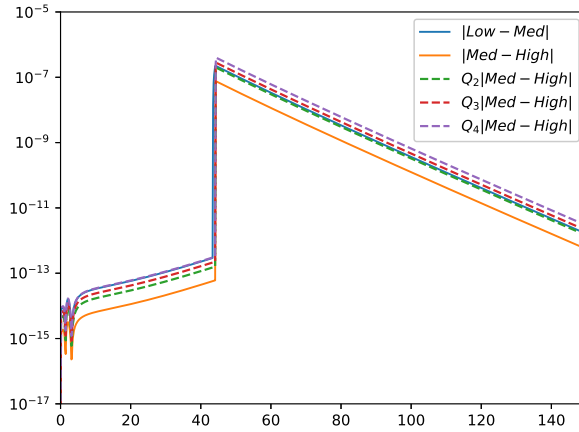


Figure 5: Convergence plot for the massive case, where Q_i for $i = 2, 3, 4$ stand for the re-scaling factor for the respective convergence rates.

References

- [1] Thibault Damour and Gilles Esposito-Farese. Nonperturbative strong field effects in tensor - scalar theories of gravitation. *Phys. Rev. Lett.*, 70:2220–2223, 1993.

- [2] D. Gerosa, U. Sperhake, and C. D. Ott. Numerical simulations of stellar collapse in scalar-tensor theories of gravity. *Class. Quant. Grav.*, 33(13):135002, 2016.
- [3] G. L. Comer and Hisa-aki Shinkai. Generation of scalar - tensor gravity effects in equilibrium state boson stars. *Class. Quant. Grav.*, 15:669–688, 1998.